Focal mechanism of the Kaliningrad earthquake of 21 September 2004 based on waveform inversion using a limited number of stations

Valerijs Nikulins, Dmytro Malytskyy*

Abstract. The focal-mechanism solution for the second shock of the Kaliningrad earthquake on 21 September 2004 (13:32 UTC) with a magnitude of Mw 5.2 was obtained using the waveform inversion (WFI) method. The method was used with the aim of its subsequent application as a discriminator in the East Baltic region for recognizing the genesis of seismic events based on data from a limited number of stations. The WFI method was tested by broadband channels. The results of focal-mechanism solution (strike = 119°; dip = 73°; rake = −163°) allowed (1) to state the source mechanism as a right-lateral strike-slip, (2) to estimate the optimal source depth equal to 3.0 km, and (3) to estimate the parameters of the compression axes (P_{az} = 340°; P_{pl} = 29°), tension (T_{az} = 252°; T_{pl} = 1°) and the axis coinciding with the intersection of two nodal planes (B_{az} = 162°; B_{pl} = 66°). These results are in satisfactory agreement with the results of the leading seismological agencies. Seismotectonic analysis showed that the epicentre of the earthquake is located inside the structure formed by the *Yantarnensk* fault zone and the zone of the *Bakalinsk* ruptured flexure. The WFI method showed its potential use as a discriminator of the genesis of seismic events.

Keywords: East Baltic region; seismic moment tensor; seismotectonic analysis; strike; dip; rake; compression; t ension; nodal plane; point source; direct waves

✉ *Valerijs Nikulins (valerijs.nikulins@lvgmc.lv; seismolat@gmail.com), Latvian Environment, Geology and Meteorology Center, Riga, Latvia; Dmytro Malytskyy (dmalytskyy@gmail.com), Carpathian Branch of Subbotin Institute of Geophysics, National Academy of Sciences of Ukraine, Ukraine*
*Corresponding author at Latvian Environment, Geology and Meteorology Center, Maskavas Street 165, LV-1019, Riga, Latvia. Email: valerijs.nikulins@lvgmc.lv; seismolat@gmail.com

INTRODUCTION

The focal-mechanism solution is important for understanding the direction and action of tectonic forces and trends in the development of geodynamic processes. In addition, the earthquake source mechanism can also be used as a discriminator to determine the genesis of a seismic event. This is due to the fact that a man-made explosion is a source that emits energy in all directions (centre of expansion), while the tectonic earthquake source is a movement along a fault and is characterized by a set of three characteristic parameters: strike, dip and rake.

In seismically active regions, determining the focal mechanism for strong earthquakes is a standard procedure. In weakly seismic, intraplate regions, with a sedimentary cover, the possibility of the focal-mechanism solution is more problematic due to small earthquake magnitudes, a rare network of seismic stations, and unfavourable geological conditions. The unfavourable geological conditions include reflecting seismic boundaries (Nikulins 2020), which are sources of seismic waves. The interference of these waves leads to a weakening of the useful signal and the difficulty of identifying the first P- and even S-waves against the background of microseisms. The geological conditions of the East Baltic region (EBR) are characterized by just such features.

The possibility of estimating of the earthquake focal mechanism in the EBR appeared relatively recent-

ly. Until the 1960s, a few modern seismographs were installed in Scandinavia. Nevertheless, for the earthquake of 25 October 1976 with M 4.7 on Osmussaar Island in the Estonian shelf zone (Kondorskaya *et al.* 1988), it was possible to determine the earthquake focal mechanism. This intraplate earthquake was mainly of the strike-slip type, but contained a significant part of reverse dip-slip faulting, possibly amounting to up to half the strike slip (Slunga 1979).

After this, several short-period stations were installed in the EBR countries without a single processing centre. The need for seismological monitoring in the EBR was mainly dictated by the safety of energy facilities – NPP (Ignalina, Leningrad), HPP (Plavinas) and others.

The possibility of assessing the earthquake focal mechanism in the EBR appeared only in 2004, after the Kaliningrad earthquakes of 21 09 2004 (Gregersen *et al.* 2007). The focal mechanism of the first earthquake (11:05 UTC) with Mw 5.0 was estimated by two seismological agencies (ETH Zurich, MEDNET Regional Centroid - Moment Tensors, Italy). The focal mechanism of the second, main shock (13:32 UTC) was estimated by a significantly larger number of seismological agencies.

The objectives of these studies were to test the method of WFI for getting a seismic moment tensor using direct P- and S-waves for the second shock of the Kaliningrad earthquake of 21 09 2004 (13:32 UTC) with M*w* 5.2. The choice of direct waves is due to the fact that these waves are less sensitive to the choice of the medium's velocity model that increases the accuracy and reliability of the method. On the basis of direct modelling, a numerical method is proposed for inverting the observed waveforms to obtain the components of the seismic moment tensor $\mathbf{M}(t)$.

In the future, it is planned to use the WFI method to recognize the genesis of seismic events in the EBR. Currently, the genesis of seismic events in the EBR is not sufficiently reliably identified by other methods.

GEOLOGICAL AND TECTONIC SETTING AND SEISMICITY

The geology of the Kaliningrad region is represented by Proterozoic and Phanerozoic formations of various composition and genesis. Early Proterozoic formations form the crystalline basement. The Phanerozoic sedimentary cover is represented by a complex of various stratigraphic deposits, with the exception of Carboniferous and Vendian.

Information on the deep geological structure of the earth's crust and upper mantle was obtained from the results of Deep Seismic Sounding (DSS) carried out in 1986 on the Sovetsk–Riga–Kohtla–Yarve geotraverse (Ankudinov *et al.* 1991). The south-western part of the DSS profile is directly adjacent to the north-eastern part of the Kaliningrad region (Sovetsk – south-western Lithuania). The thickness of the earth's crust there reaches 40–45 km, and the surface of Moho is almost horizontal.

Later studies of the deep structure of the earth's crust and upper mantle were carried out in 1995 along the EUROBRIDGE profile (Eurobridge'95 seismic working group, 2001), which crosses the land area from northwest to southeast, from the Baltic Sea to the border with Belarus. The nearest sections of the profile are located approximately 140 km from Kaliningrad. According to these studies, the most significant feature of the velocity section of the earth's crust is the presence of a layer of low velocities in the depth interval of 8–12 km. In this depth range, the P-wave velocity decreases to 6.15 km/s, while above and below it reaches the values of 6.25–6.35 km/s.

The microseismic sounding method (MSM), based on the phenomenon of distortion of the microseismic field in the vicinity of velocity inhomogeneity (Gorbatikov *et al.* 2008), was important for understanding the spatial position of the Kaliningrad earthquake source. Two profiles crossing the Pregol fault zone (eastern Kaliningrad), as well as the Yantarnensk fault zone and the zone of the Bakalinsk ruptured flexure (southwest–northeast direction) showed the presence of subvertical zones of low velocities (ZLV) at a depth interval of 8–22 km (Rogozhin *et al.* 2014). The upper part of this zone is isolated at a depth interval of 8–12 km. This part of the ZLV corresponds to the same zone traced within the Baltic syneclise on the EUROBRIDGE Deep Seismic Sounding (DSS) profile (Eurobridge'95 seismic working group, 2001).

According to DSS obtained from profiles in the Baltic Sea and on the eastern coast of Sweden (Fennolora, the Babel and Baltic Sea profiles), a depression of the Moho boundary with stepped boundaries 2–3 km high on both sides was discovered (Ostrovsky *et al.* 1994). The Moho depression is about 110 km wide, and its southern edge is located about 110 km from the northern coast of the Sambia Peninsula. In the section of the earth's crust, according to the velocities of seismic waves, three layers are distinguished, and all three layers are curved above the depression. This depression is also traced on the Fennolora and Babel seismic sounding profiles. The reduced velocity of P-waves in the upper mantle under the depression of the Moho boundary was as an argument for the assumption of the existence of a rift zone in the Baltic Sea (Ostrovsky 1995). The rift zone is oriented approximately along an azimuth of 120°. The length of the discovered rift zone is at least 500 km, from the coast of Sweden to the Kaliningrad region of Russia. Thus, the discovery of an ancient rift zone beneath the central part of the Baltic Sea is an important argument

in understanding the complex history of geodynamic development of the Baltic region.

Within the Sambia Peninsula, the depth of the crystalline basement increases from east to west and southwest from 2400 m to 2900 m, and up to 3000 m in the shelf zone. The Kaliningrad uplift is located in the central part of the Sambia Peninsula and then continues in the shelf zone. Within its limits, the amplitude of displacement along faults reaches 70–130 m (Lukyanova et al. 2011).

From the tectonic point of view, the Sambia Peninsula, like the entire Kaliningrad region, is located in the south-eastern part of the West Lithuanian Granulite Massif, on the outskirts of the East European Craton. It is located between the Teisseyre-Tornquist suture zone and the Neman system of active fault dislocations (Bogdanova et al. 1994). Several stages of development are distinguished in the sedimentary cover: Caledonian, Early Hercynian, Late Hercynian, Cimmerian, and Alpine.

The total thickness of the structural complexes on land and sea differs significantly. The thickness of the Caledonian structural complex varies from 600 m in the east to 2000 m in the west within the water area.

According to the scheme of tectonic zoning of the territory of the Kaliningrad region (Otmas et al. 2006) based on a structural map of the surface of the Caledonian complex of the sedimentary cover (top of the Ordovician), the main elements are the Northern Sambia Depression, West Curonian Shaft, Zelenogradsk Depression, Sambia Rock Step, Kaliningrad Shaft, Pregol Depression, Bagrationovsk Rock Step, and Mamontovsk Depression.

The longitudinal Sambia Rock Step is located in the central part of the Sambia Peninsula. The Kaliningrad uplift is located south of the Sambia Rock Step; it also has a longitudinal strike. This is an uplifted, horst-like fault zone, within which a chain of local uplifts is located.

Quaternary deposits are widespread throughout the Kaliningrad region. They are located on the blurred surface of the Cretaceous and Paleogene. Their thickness varies from a few meters to 266 m, reaching 50–60 m on average.

The study area (Sambia Peninsula) is located near large neotectonic structures. In particular, according to the results of the international project IGCP 346 "*Neogeodynamica Baltica*", the Baltic Graben System is located in the eastern part of the Baltic Sea. It includes the East Gotland Graben, the southern part of which is represented by the Gdansk Depression, located west of the Sambia Peninsula. The total amplitudes of vertical, neotectonic movements, starting from Rupelian (Oligocene–Quaternary times, 35–37 Ma), reach – 100 m west of the Sambia Peninsula and – 200 m in the central part of the East Gotland Graben (Garetsky et al. 1999). The southern and northern edges of the East Baltic Graben are characterized by an increased horizontal gradient of the total amplitudes of neotectonic movements (HGTANM). These edges coincide with the foci of the Osmussaar (1976) and Kaliningrad (2004) earthquakes, where the HGTANM value reached 3.6 and 3.7 m / km, respectively. This can be considered the evidence of the modern inherited activity of neotectonic movements of the earth's crust, at least along the edges of the indicated neotectonic structure (Nikulins 2007). The HGTANM gradient roughly corresponds to the position of the contrasting scarps of the deformed sedimentary layers. The presence of a similar structural-denudation scarp in sedimentary rocks is also confirmed by other sources (Blazhchizhin 1974) on the western and north-western underwater slopes of the Sambia Peninsula, 5–10 km from the coast. According to the "Neotectonic Map of the Soviet Baltic Republics" (Grigelis 1981), two longitudinal neotectonically active linear zones are identified in the north and south of the Sambia Peninsula.

The territory of the peninsula is crossed by a number of lineaments, mainly of submeridional and, to a lesser extent, south-western–north-eastern striking. These lineaments, according to researchers (Lukyanova et al. 2011), are associated with recent tectonic faults and are their reflection on the modern surface. Their length sometimes exceeds a hundred kilometres.

The lower boundary of neotectonic processes refers to the beginning of the Neogene (Lukyanova et al. 2011). Tectonic ruptures are still occurring. For example, this is evidenced by the intensive formation of cracks on the asphalt surface of a road about 2 km long (Lukyanova et al. 2011) in the Gvardeisky District.

The Baltic region is characterized by a low level of seismicity, with a maximum magnitude below 6 (Gregersen et al. 2007). Most researchers (Lundqvist, Lagerback 1976; Lagerback 1979; Gregersen, Basham 1989; Slunga et al. 1989) believe that earthquakes that occur in the Baltic region are caused by tectonic pressure from the Mid-Atlantic Ridge, or post-glacial recovery of the isostatic state of crust disturbed by glacial load.

The geodynamic regime is determined by the tectonic stresses prevailing in the region. The main contribution to the assessment of the maximum horizontal stresses, according to the World Stress Map (Heidbach et al. 2010), is made by stress indicators obtained by two main methods: method based on the focal-mechanism solution (FSM) (72%) and method based on the assessment of wellbore breakouts and drilling induced fractures (BO) (20%). The contribution of other methods is much less.

According to earthquakes in southern Sweden, the azimuth of the maximum horizontal stresses S_{H_max} is located in the northwest–southeast direction (Slunga *et al*. 1984). The azimuth range corresponds to the interval of 110°–180°, and the maximum values correspond to the azimuth range of 129°–146°.

According to the World Stress Map database, in a well which is located in the Baltic Sea (BO method) the azimuth S_{H_max} was estimated at 28°. In the continental area, in northern Poland, in a well approximately 244 km southwest of the Kaliningrad earthquake there was observed a systematic rotation of azimuth S_{H_max} for the Jurassic-Triassic sequence, ranging from 150° to 170°, respectively.

Specific tectonic conditions have a significant impact on regional stresses, which are a consequence of the configuration of tectonic faults (Stephansson, Zang 2012) and factors driven by the history of geological development. Consequently, global stresses caused by pressure from the North Atlantic Ridge (spreading zone) can be "corrected" by the local stress field. In particular, a study in the East Baltic region, based on measurements of the GPS station network, identified three different provinces that exhibit different stress regimes (Zakarevičius *et al*. 2011).

An analysis of historical sources (Peter 1997; David 1813; Laska 1902) allowed Professor A. Nikonov to compile a catalogue of earthquakes (Nikonov 2007) for the Kaliningrad region (East Prussia). At the same time, according to A. Nikonov, there was not one earthquake, but 4 earthquakes in 1302. Of these, the first 3 earthquakes (φ = 55.0° N; λ = 20.0° E), with an intensity of V–VII points, were attributed to a seismic swarm, and the fourth earthquake, with a shaking intensity of VII points, occurred at a different time and had different coordinates of the epicentre (φ = 55.3° N; λ = 21.0° E). Another earthquake occurred in 1328 (φ = 55.1° N; λ = 23.5° E). At the same time, A. Nikonov notes the ambiguity of the assessment of the parameters of these earthquakes and, therefore, low reliability.

The first regional seismological studies began after the Osmussaar earthquake on 25 October 1976. They were carried out in the epicentral zone and at individual stations of the East Baltic region: Suginčiai (Lithuania), Skujas (Latvia), and Tallinn ((Estonia). However, the absence of a unified collection and analysis centre did not allow the study of regional seismicity. A network of seismic stations with a single collection centre appeared only after the 2004 Kaliningrad earthquake as part of the international network GEOFON with centre in GFZ Potsdam.

A number of researchers use data obtained from various seismological agencies: the Geophysical Service of the Russian Academy of Sciences, the Norwegian Seismic Array NORSAR, the European Mediterranean Seismological Centre (EMSC), the International Data Centre (IDC) CTBTO, the International Seismological Centre (ISC) CTBTO.

However, these data are not always reliable enough. The authors (Ulomov *et al*. 2008; Rogozhin *et al*. 2014) who use these data to assess seismic risk do not sufficiently critically assess their reliability. This can affect the seismic risk assessment.

There are two main reasons why many of the data in the catalogues and bulletins of the above international agencies are identified as earthquakes. The first reason is associated with a large number of technogenic sources both in the continental part of the East Baltic region and in the Baltic Sea, as well as with the difficulty of determining the genesis of a seismic event (Nikulins 2020) due to geological conditions and microseismic background. The second reason is associated with the historical seismic events of 1908 in the Eastern Baltic region. They mistakenly refer to earthquakes, while a number of studies (Nikonov 2010; Nikulins 2017) have shown their connection with frost phenomena (cryoseisms).

REVIEW OF RESEARCH ON LOCALIZATION AND FOCAL-MECHANISM SOLUTION

There is a significant scatter in the results of localization of the second Kaliningrad earthquake on 21 September 2004 (Fig. 1).

Figure 1 shows the epicenters of the second shock of the Kaliningrad earthquake of 21 September 2004 identified by international seismological agencies and leading experts, as well as the results of localization according to Latvian Environment Geology and Meteorology Centre (LEGMC) data (Table 1). Figure 3 was created on the basis of the fault tectonics scheme and the surface relief of pre-Quaternary rocks in the Kaliningrad region (Rogozhin *et al*. 2014). The original is based on the materials of Zagorodnyh *et al*. (2002) on geological and ecological research and mapping of the territory of the Kaliningrad region and the materials of Dodonov *et al*. (1976).

This earthquake had several characteristic features. First, according to the results of instrumental localization by 22 agencies and leading experts, there is noticeable large dispersion in the position of the epicentre (Fig. 1). Three areas of compact location of epicentres for the second earthquake can be distinguished. According to data from 5 agencies (1, 2, 10, 16, 17), the epicentre is located northeast and north of the zone of Bakalinsk ruptured flexure. Most of the epicentres, according to 9 agencies (5, 6, 7, 8, 12, 14, 19, 20, 21), are concentrated within or at the edge of the tectonic zone formed by the Yantarnensk fault zone and zone of the Bakalinsk ruptured flexure.

These zones are parallel to each other. The strike
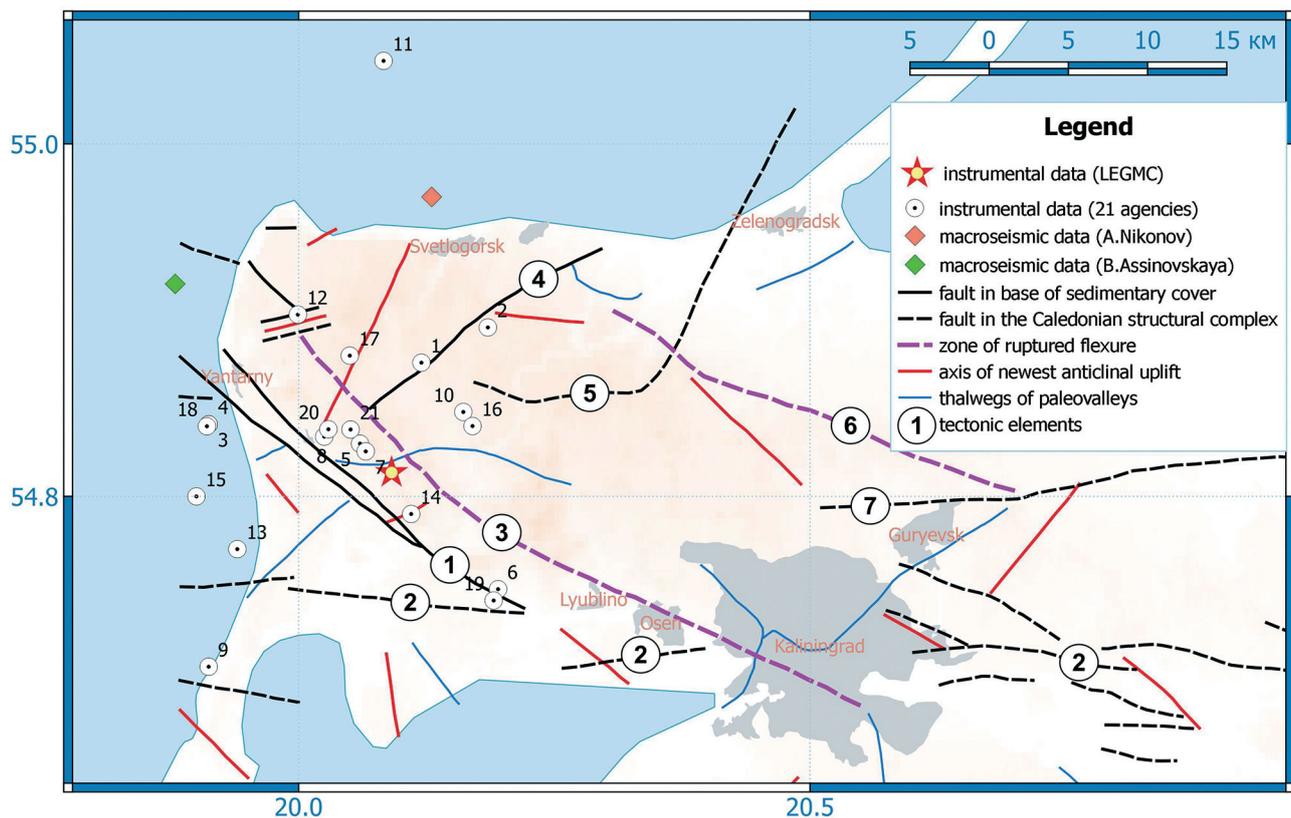
Fig. 1 Results of localization of the epicenter of the second (13:32 UTC), the main shock of the Kaliningrad earthquake on 21 September 2004 and tectonic setting of the study area (tectonic framework is after Rogozhin *et al.* (2014)). Names of tectonic elements: 1 –Yantarnensk fault zone; 2 – Pregol fault zone; 3 – zone of Bakalinsk ruptured flexure; 4 – Pionersk fault; 5 – Zelenograd fault; 6 – Melnikovsk flexure complicated by ruptures; 7 – Gusev fault

azimuths of these tectonic elements are approximately 127°–138°. These faults are close in strike azimuth to the Teisseyre – Tornquist Zone (azimuth approximately 114°–116° (Mazur *et al.* 2015)) separating the ancient, Precambrian East European Craton from the younger Phanerozoic orogen of south-western Europe. According to six agencies (3, 4, 9, 13, 15, 18), the earthquake's hypocentre is located in the west of the offshore zone of the Sambia Peninsula.

Second, there is a significant difference between the position of the epicentre according to instrumental and macroseismic data. The epicentre of the second, main shock of the earthquake according to macroseismic data is located either in the northern offshore zone of the Sambia Peninsula (Nikonov 2007) or in the western (Assinovskaya 2009). A later version of localization, according to Assinovskaya *et al.* (2011), showed the closeness of macroseismic and instrumental results in the shelf zone in the west of the Sambia Peninsula.

Third, seismic deformations on the earth's surface, located on the eastern and northern shores of the pond near Veselovka city (Aptikaev *et al.* 2019), are located within the seismogenic zone formed by the Yantarnensk fault zone and the zone of the Bakalinsk ruptured flexure.

MATERIALS AND METHODS

Seismic network and hypocentre localization

The Kaliningrad earthquakes of 21 09 2004 were registered at many seismic stations in Europe and at some stations in the world. To localize the second shock of the Kaliningrad earthquake (13:32 UTC) there were used the closest to the hypocentre earthquake and accessible stations of the GEOGON GFZ Potsdam network (KWP, MORC, RGN, RUE, VSU, PUL), Poland (SUW) and Russia (OBN). To calculate the seismic moment tensor, the broadband channels (BH*) of the SUW, VSU, RGN and RUE stations were used. Figure 2 shows the stations that were used to localize the hypocentre of the second shock (09 21 2004 13:32 UTC) of the Kaliningrad earthquake (KWP, MORC, OBN, RGN, RUE, SUW, VSU), other stations of the GEOFON network and of national networks in the East Baltic region (PUL, SLIT, PABE, PBUR) and stations used to the focal-mechanism solution by the WFI method. A velocity model was used based on the DSS results along the *EUROBRIDGE* profile (Janutyte *et al.* 2013). The uneven distribution of stations around the earthquake epicentre could affect the quality of localization of the earthquake hypocentre.

The peculiarity of the localization of the hypocen-

Table 1 Parameters of localization of the hypocentre of the second shock of the Kaliningrad earthquake on 21 September 2004 (13:32) which were identified by international seismological agencies and experts

Origin Time	Lat	Lon	H, km	Mag	Mag type	Agency	No fig. 1	No. of stations
13:32:31.0	54.876	20.120	20	5.2	Mw	IGF	1	65
13:32:28.3	54.896	20.185	10	5.1	mb	GS RUS	2	42
13:32:30.0	54.841	19.912	15	4.7	Mw	ETHZ	3	31
13:32:30.8	54.841	19.912	10	4.9	mb	NEIC	4	112
13:32:30.8	54.83	20.50	20.5	4.7	Mw	MED-NET	5	19
13:32:29.3	54.747	20.195	10	5.3	Ml	LDG	6	
13:32:30.1	54.826	20.066	0	4.9	Ml	CTBTO	7	35
13:32:31.9	54.834	20.025	10	5.0	Ml	HEL	8	36
13:32:32.7	54.703	19.912	10	5.4	Ml	BGR	9	19
13:32:33.7	54.848	20.161	10	5.4	Ml	BER	10	13
13:32:34.1	55.047	20.083	10.3	5.4	Ml	NAO	11	8
13:32:28.5	54.903	19.999	1.2	4.8	mb	ISC	12	352
13:32:29.2	54.77	19.94	10	5.0	mb	EMSC	13	
13:32:30.8	54.79	20.11	20.2	4.9	mb	GCMT	14	40
13:32:29.2	54.8	19.9	10			ORFEUS	15	
13:32:31.3	54.84	20.17	17	5.1	mb	GAB	16	65
13:32:30.8	54.88	20.05	8.4			ASS	17	26
13:32:30.8	54.84	19.91	10	4.8		IRIS	18	
13:32:29.3	54.74	20.19	10			STR	19	11
13:32:32.3	54.838	20.029	20.2			EHB	20	336
13:32:32.3	54.838	20.051	20.2			ISC-EHB	21	305
13:32:31.3	54.813	20.091	10	5.6	mb	LEGMC	*	8

*Denotations: IGF – Poland Institute of Geophysics; GS RUS – Geophysical Survey of the Russian Academy of Sciences; ETHZ – Seismology and Geodynamics (SEG) group at ETH Zurich; NEIC – National Earthquake Informational Centre (USGS); MEDNET – Mediterranean Very Broadband Seismographic Network; LDG – CEA Laboratory of Detection and Geophysics; CTBTO – International Data Centre of Comprehensive Nuclear-Test-Ban Treaty Organization; HEL – Institute of Seismology of the University of Helsinki; BGR – Federal Institute for Geosciences and Natural Resources; BER – University of Bergen; NAO (NORSAR) – Norwegian Seismic Array; ISC – International Seismological Centre; EMSC – European Mediterranean Seismological Centre; GCMT –The Global CMT Project; LDEO – Lamont Doherty Earth Observatory, (Columbia University); ORFEUS – Observatories & Research Facilities for European Seismology; GAB – localization according to I. Gabsatarova (Russia); ASS – localization according to B. Assinovskaya (Russia); IRIS – Incorporated Research Institutions for Seismology; STR – EOST/ReNaSS – Strasbourg Cedex, France; EHB – Physics Department, University of Colorado, Boulder, Co. USA (B.Engdahl); * – Latvian Environment, Geology and Meteorology Centre.*

tre was the difficulty in identifying the S-wave. The maximum amplitude in the S-wave group was attributed to Lg waves, the occurrence of which is due to the superposition of multiple S-wave reverberations and SV to P transformations and/or vice versa, P to SV transformations within the entire earth's crust. Localization was done by the first P-waves and S-waves.

Waveform inversion method

Currently, moment tensors are calculated by several approaches: using amplitudes of seismic waves (Vavrychuk, Kuhn 2012; Godano *et al*. 2011), S/P amplitude ratios (Hardebeck, Shearer 2003), or full waveforms (Mai *et al*. 2016; Weber 2006, 2016). The inversion of full waveforms is a widely used approach applicable on all scales: from small to large earthquakes. Ferdinand, Arvidsson (2002) used an interactive inversion approach to demonstrate the retrieval of the source parameters of three small earthquakes and developed a modified model of structure

along the propagation path. Moment tensor inversion was carried out by minimizing the L2 norm of the difference between synthetic and observed displacement data under a deviatoric condition. Results for the three small earthquakes showed good agreement between single station and multistation source solutions.

In this study, a method is presented for moment tensor inversion of only direct P- and S-waves, which are less sensitive to path effects modelling than reflected and converted waves, which significantly improves the method' accuracy and reliability. Based on forward modelling, a numerical technique is developed for the inversion of observed waveforms for the components of the moment tensor $M(t)$, obtained by generalized inversion. Addressing the problem of unavoidable inaccuracy of seismic waves modelling, we propose to invert only the direct P- and S-waves instead of the full field. The advantage of inverting only the direct waves consists in their much lesser distortion, if compared to reflected and converted waves, by inaccurate modelling of velocity contrasts.

Fig. 2 Seismic stations of the GEOFON network, stations of national seismic networks used for the localization and of the Kaliningrad earthquake's focal-mechanism solution

Thus, the direct waves, consequently, have a much less distorted imprint of the source. The advantage, in this connection, of choosing the matrix method for the calculation of the wave field consists in its ability to analytically isolate only the direct waves from the full field.

A method, presented here enables one to obtain the focal-mechanism solution by inversion of waveforms recorded at a limited number of seismic stations. The inversion scheme consists of two steps. First (forward modelling), propagation of seismic waves in vertically inhomogeneous media is considered and a version of the matrix method for calculation of synthetic seismograms on the upper surface of the horizontally layered isotropic medium is developed. The point source is located inside a layer and is represented with a seismic moment tensor. The displacements on the upper surface are presented in matrix form in the frequency and wave number domain, separately for the far-field and the near-field (Malytskyy 2010, 2016; Malytskyy, Kozlovskyy 2014; Malytskyy, D'Amico 2015). Subsequently, only the far-field displacements

are considered and the wave-field from only direct P- and S-waves is isolated with application of eigenvector analysis reducing the problem to system of linear equations (Malytskyy 2016). Subsequently (inverse modelling), spectra of the moment tensor components are calculated using a solution of generalized inversion and transformed to time domain by applying the inverse Fourier transform.

Forward modelling

Assuming that the point source, represented by a symmetric moment tensor $M(t)$, is located within a stack of solid, isotropic, homogeneous, perfectly elastic layers with horizontal and perfectly contacting interfaces, the layers characterized by thickness, density, and velocities of P- and S-waves, the following expressions have been obtained by Malytskyy (2010, 2016) in cylindrical coordinates for the displacements $u_z^{(0)}(t, r, \varphi)$, $u_r^{(0)}(t, r, \varphi)$, and $u_\varphi^{(0)}(t, r, \varphi)$ on the upper surface of the half-space at $z = 0$:
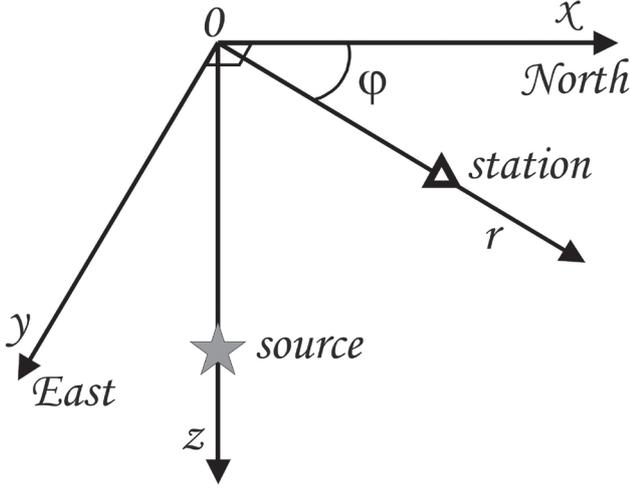
Fig. 3 Cylindrical and Cartesian coordinates of the source and the station

$$\begin{pmatrix} u_z^{(0)} \\ u_r^{(0)} \end{pmatrix} = \sum_{i=1}^{3} \int_0^\infty k^2 \mathbf{I}_i L^{-1} \left[m_i \mathbf{g}_i \right] dk ,$$

$$u_\varphi^{(0)} = \sum_{i=5}^{6} \int_0^\infty k^2 J_i L^{-1} \left[m_i g_{\varphi i} \right] dk ,$$ (1)

where

$$m_1 = M_{xz}\cos\varphi + M_{yz}\sin\varphi , \quad m_2 = M_{zz} ,$$

$$m_3 = \cos^2\varphi \cdot M_{xx} + \sin^2\varphi \cdot M_{yy} + \sin 2\varphi \cdot M_{xy} ,$$

$$m_4 = -\cos 2\varphi \cdot M_{xx} + \cos 2\varphi \cdot M_{yy} - 2\sin 2\varphi \cdot M_{xy} ,$$ (2)

$$m_5 = M_{yz}\cos\varphi - M_{xz}\sin\varphi ,$$

$$m_6 = \sin 2\varphi \cdot M_{xx} - \sin 2\varphi \cdot M_{yy} - 2\cos 2\varphi \cdot M_{xy}$$

M_{xx}, M_{xy},…, M_{zz} are the Cartesian components of the moment tensor $M(\omega)$ representing the source located at $r = 0$, axis x pointing North and y East, φ is the station's azimuth (Fig. 3), k is the horizontal wave number, functions $\mathbf{g}_i = (g_{zi}, g_{ri})^T$, and $g_{\varphi i}$ contain propagation effects between the source and the receiver (Malytskyy 2010, 2016),

$$\mathbf{I}_1 = \begin{pmatrix} J_1 & 0 \\ 0 & J_0 \end{pmatrix}, \ \mathbf{I}_2 = \begin{pmatrix} J_0 & 0 \\ 0 & J_1 \end{pmatrix},$$

$$\mathbf{I}_3 = \mathbf{I}_2 , \ J_5 = J_0 , \ J_6 = J_1$$ (3)

are the Bessel functions of argument kr, and L^{-1} is the inverse Laplace transform, from frequency to time domain.

Further, only the far-field displacements are considered and the wave-field from only direct P- and S-waves is isolated with application of eigenvector analysis reducing the problem to system of linear equations (Malytskyy 2016). Equation (1) is then expressed in matrix form for only the direct P- and S-waves on the upper surface of the half-space in frequency and wave number domain (ω, k) (Malytskyy 2010):

$$\mathbf{U}^{(0)} = \mathbf{K} \cdot M$$ (4)

where vector $\mathbf{U}^{(0)} = (U_x^{(0)P}, U_x^{(0)S}, U_y^{(0)P}, U_y^{(0)S}, U_z^{(0)P}, U_z^{(0)S})^T$ contains the six Cartesian displacement components of direct P- and S-waves, vector $M = (M_{xz}, M_{yz}, M_{zz}, M_{xx}, M_{yy}, M_{xyz})^T$ consists of the six independent Cartesian components of moment tensor $\mathbf{M}$, matrix $\mathbf{K}$ accounting for path effects and transformations between the Cartesian and cylindrical coordinates:

$$\mathbf{K} = \begin{pmatrix} K_{11}^P & K_{12}^P & K_{13}^P & K_{14}^P & K_{15}^P & K_{16}^P \\ K_{21}^S & K_{22}^S & K_{23}^S & K_{24}^S & K_{25}^S & K_{26}^S \\ K_{31}^P & K_{32}^P & K_{33}^P & K_{34}^P & K_{35}^P & K_{36}^P \\ K_{41}^S & K_{42}^S & K_{43}^S & K_{44}^S & K_{45}^S & K_{46}^S \\ K_{51}^P & K_{52}^P & K_{53}^P & K_{54}^P & K_{55}^P & K_{56}^P \\ K_{61}^S & K_{62}^S & K_{63}^S & K_{64}^S & K_{65}^S & K_{66}^S \end{pmatrix} .$$ (5)

When only the direct P-waves are used, matrix $\mathbf{K}$ reduces to

$$\mathbf{K}^P = \begin{pmatrix} K_{11}^P & K_{12}^P & K_{13}^P & K_{14}^P & K_{15}^P & K_{16}^P \\ K_{21}^P & K_{22}^P & K_{23}^P & K_{24}^P & K_{25}^P & K_{26}^P \\ K_{31}^P & K_{32}^P & K_{33}^P & K_{34}^P & K_{35}^P & K_{36}^P \end{pmatrix} .$$ (6)

Thus, Eq. (4) can be written only for the direct P-waves in matrix form:

$$\mathbf{U}^{(0)P} = \mathbf{K}^P \cdot M,$$ (7)

where $\mathbf{U}^{(0)P} = (\mathbf{U}_x^{(0)P}, \mathbf{U}_y^{(0)P}, \mathbf{U}_z^{(0)P})^T$ defines the observed amplitudes of the direct P-waves, and the components of matrix $\mathbf{K}^P$ in accordance with Malytskyy (2016).

Inversion modelling

Now, that a direct relation between the moment tensor and the displacements on the free surface of the half-space is defined by Eq. (7), the moment tensor can be determined from the displacements by inverting the relation.

A least-squares solution to the over-determined system of Eq. (7) for M (for there are $3 \times k \times \omega$ equations in total for $6 \times \omega$ unknowns) can be obtained by generalized inversion (Aki, Richards 1980):

$$M = (\tilde{\mathbf{K}}^P \mathbf{K}^P)^{-1} \tilde{\mathbf{K}}^P \mathbf{U}^{(0)P} ,$$ (8)

where the tilda denotes complex conjugation and transposition, and -1 inversion and $(\tilde{\mathbf{K}}^P \mathbf{K}^P)^{-1}\tilde{\mathbf{K}}^P$ is the generalized inverse of $\mathbf{K}^P$.

Thus, since all the six independent components of moment tensor M contribute to the waveforms $U^{(0)}$ at only one station in the over-determined system of Eq. (7), the inversion scheme of Eq. (8) should enable, at least theoretically, to obtain a unique solution for each of them. Within the limitations of the current source presentation and path effects modelling, the solution is exact and convergence is reached after a single

iteration. The inverse problem in this case consists of determining the parameters of point source under the condition that the source location and origin time is known, as well as the distribution of velocities of seismic waves between the source and the station. Eq. (7) is expressed in matrix form for direct P- waves at N stations ($i = 1,…, N$) in the spectral domain:

$$GM = U_n^{(0)p} \qquad (9);$$

$$G = \begin{pmatrix} K_1 \\ \vdots \\ K_N \end{pmatrix} \qquad (10);$$

$$U_n^{(0)p} = (U_1^{(0)p}, U_2^{(0)p}, …, U_N^{(0)p})^T \qquad (11)$$

The vector M of moment time functions is obtained using the generalized inversion:

$$\bar{M} = (\tilde{G}^*G)^{-1}\tilde{G}^*U_n^{(0)p} \qquad (12)$$

RESULTS

As a result of localization by LEGMC (Fig. 1), the epicentre of the earthquake was inside the tectonic structure formed by the Yantarnensk fault zone and the zone of the Bakalinsk ruptured flexure. Most seismological agencies have also located the epicentre of the earthquake within this structure. The Yantarnensk fault zone penetrates the base of sedimentary cover (Caledonian structural complex), and the zone of the Bakalinsk ruptured flexure is associated to the Alpine stage. The Pregol fault zone and adjacent tectonic structures currently show signs of activity. These include a striking manifestation of linear uplift throughout the Holocene. Flexures are expressed exclusively by folded deformations in Holocene sediments and landforms (Rogozhin *et al*. 2014). Thus, the association of the epicentre of the Kaliningrad earthquake to these zones confirms their modern tectonic activity.

As a result of applying the WFI method to estimate the parameters of the focal mechanism of the considered Kaliningrad earthquake, the focal-mechanism solutions were obtained for two and four seismic stations. When using 2 stations (SUW and VSU), the following parameters of the focal mechanism were obtained: nodal plane 1 – strike = 108°; dip = 66°; rake = -166°. When using 4 stations (SUW, VSU, RGN, and RUE), parameters of the focal mechanism were as follows: nodal plane 1 – strike = 119°; dip = 73°; rake = -163°. The parameters of the nodal planes differ insignificantly, but the focal mechanism remains unchanged – right-lateral strike-slip. These test cases have shown that in low seismicity conditions an estimate of the focal mechanism parameters can be obtained using a limited number of seismic stations. However, the 4-station variant is preferred.

In this case, the strike azimuth of the nodal plane better corresponds to the strike azimuth of the tectonic elements forming the above tectonic structure, as well as close in strike to the Teisseyre–Tornquist zone.

The earthquake focal mechanism, regardless of the number of stations used, corresponds to a right-lateral strike-slip. Assessment parameters of the tectonic stresses gave the following results: for the compression axis P, strike azimuth P_{az} = 340°, plunge angle P_{pl} = 29°; for the tension axis T, strike azimuth T_{az} = 252°, plunge angle T_{pl} = 1°; strike azimuth for the axis coinciding with the intersection of two nodal planes B_{az} = 162°, plunge angle B_{pl} = 66°.
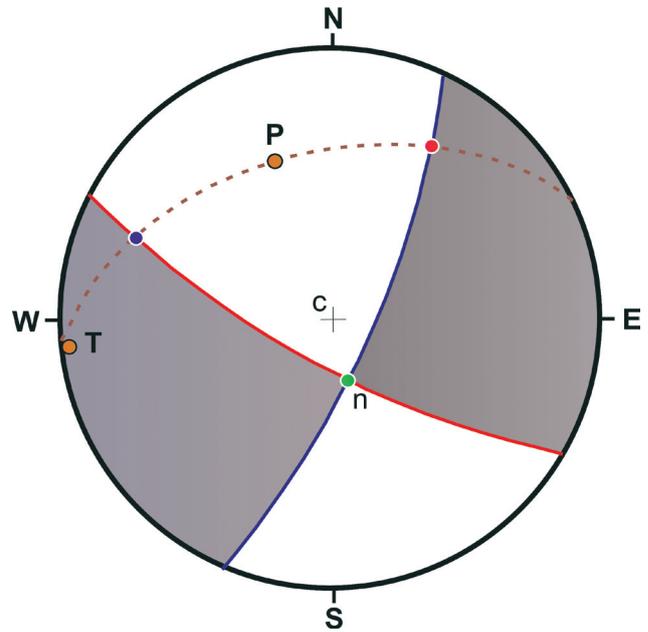
Fig. 4 Focal mechanism of the Kaliningrad earthquake on 21 September 2004 (13:32 UTC): c is centre of diagram; n is point of intersection of nodal planes; P is point of application of the compression axis; T is point of application of the tension axis; the dotted line is the plane of poles; the red line is preferred nodal plane

The WFI method also made it possible to determine the time at the source of the earthquake (t_0 = 13:32:30), that is, to determine the onset of the earthquake and the time function of the source (STF). According to the authors, the definition of STF(t) can be used for early warning, which will be investigated by the authors in subsequent works.

Thus, the studies have demonstrated the main advantage of the WFI method, that is, the ability to estimate the parameters of the earthquake focal mechanism using a limited number of broadband seismic stations. The WFI method can be used as a discriminator of genesis of seismic events in the EBR, since other discriminators have not yet demonstrated unambiguity (Fourier spectra, ratios of spectra or amplitudes of P- and S-waves, time-frequency analysis) and efficiency (Nikulins 2017), or insufficiently studied

(the complex index for assessing the integral power of S- and P-waves – complexity index), or have not yet been tested (SOM – Self Organized Map).

DISCUSSION

A comparison of the results of solving the focal mechanism of the second Kaliningrad earthquake on 21 September 2004 (13:32 UTC), obtained in this study, with the results of the solution of four other seismological agencies is shown in Table 2. These solutions of the focal mechanism of the Kaliningrad earthquake are based on use routine determination of focal mechanisms obtained from first motion P-wave arrivals (Lentas 2018; Lentas *et al.* 2019) and published in the International Seismological Centre.

It can be seen that the results of the focal-mechanism solution for several agencies (MED_RCMT, GCMT, IGF) are quite close to the results of solving the focal mechanism in this study. Only the ZUR_MRT results show a strike-slip faulting with a minor thrust component. Dark background in Table 2 shows the nodal planes of preferred solutions for the focal mechanism of the second Kaliningrad earthquake. Their orientation to a greater extent corresponds to the orientation of tectonic elements of the Yantarnensk fault zone and the zone of the Bakalinsk ruptured flexure.

The results of orientation of the main stress axes P, T obtained in this study are in satisfactory agreement with the results by GCMT. Estimates of the coseismic strain field for the Kaliningrad earthquake of 21 September 2004 showed practically the same values of the maximum compression and maximum dilatation (Assinovskaya *et al.* 2011). In the area of the Sambia Peninsula, the compression axis is oriented approximately in the north-south direction, and the extension axis in the west-east direction.

GCMT used 40 seismic stations, and IGF probably

no less than 6 seismic stations. In the research of the authors, 4 seismic stations were used. The EBR with a low level of seismicity is characterized by seismic events with small magnitudes, not exceeding 2.5–2.7. Therefore, if there is a need and opportunity to assess the source mechanism of an earthquake in EBR, then, as a rule, many seismic stations cannot be used. The WFI method will assess the source mechanism of seismic events in EBR for small magnitudes and a limited number of stations.

In the WFI method, the results of the earthquake focal-mechanism solution depend on the choice of the focal depth. Therefore, the focal depth was varying from 1 to 20 km. In this case, the focal mechanism radically changes from a normal fault mechanism to a right-lateral strike-slip mechanism.

Due to the large epicentral distances, the reliability of determining the depth of the hypocentre is low. This is confirmed by the spread of the hypocentre depth (from 0 km to 20.5 km) according to world agencies and experts (Table 1). At a focal depth of 3.0 km, the earthquake focal-mechanism solution is most consistent with the results of the solution of the world's leading agencies. The azimuth of the compression axis P falls within the range of S_{H_max} values in the continental Baltic region (northern Poland) and is close to the azimuths S_{H_max} for the south of Sweden (see the section "Geological and tectonic setting and seismicity"). Among the seismological agencies that determined depths less than 3.0 km, there were only ISC (1.2 km) and CTBTO (0.0 km).

CONCLUSIONS

In this study, a WFI method is presented for moment tensor inversion of only direct P- and S-waves recorded by a limited number of seismic stations. The method is based on an inversion approach (described in Malytskyy 2010, 2016), where a version of the matrix

Table 2 Comparative results of the focal-mechanism solution of the second shock of the Kaliningrad earthquake of 21 09 2004 (13:32 UTC). Designations: ZUR_RMT – Swiss Seismological Service; MED_RCMT – Med-Net Regional Centroid Moment Tensor project; GCMT – HRVD/GCMT, The Global CMT Project; IGF – Poland Institute of Geophysics; Mal & Nik – authors of this study; Az – azimuth; Pl – plunge; Num st. – number of seismic station; P, T, B – see Fig. 4

Agency	Plane	Strike	Dip	Rake	H, km	P		T		B		No st.
						Az	Pl	Az	Pl	Az	Pl	
ZUR_RMT	1	26.0	86.0	26.0	15.0	157	15	253	21	33	64	
	2	294.0	64.0	176.0								
MED_RCMT	1	211.0	85.0	-8.0	20.5	166	9	257	3	3	80	19
	2	302.0	82.0	-175.0								
GCMT	1	22.0	83.0	-5.0	20.2	338	8	247	1	148	82	40
	2	113.0	85.0	-173.0								
IGF	1	204.7	84.3		20.0							
	2	113.4	77.3									
Nik & Mal	1	119.0	73.0	-163.0	3.0	340	29	252	1	162	66	4
	2	23.0	73.0	-17.0								

method has been developed for the calculation of direct waves in the horizontally layered half-space from the point source represented by its moment tensor.

Evaluation of the focal mechanism parameters for the second shock of the Kaliningrad earthquake of 21 09 2004 (13:32 UTC) showed that the applied WFI method is promising for determining intraplate earthquakes with relatively small magnitudes in regions with a low level of seismicity and a limited number of seismic stations. The main advantage of the method is in its application to solve the earthquake focal mechanisms in the low seismic activity East Baltic region.

The focal mechanism of the second shock of the Kaliningrad earthquake was estimated as right-lateral strike-slip faulting. Parameters of preferred nodal plane 1 are as follows: strike = 119°; dip = 73°; rake = -163°, and parameters of tectonic stresses are as follows: for the compression axis P, strike azimuth $P_{az} = 340°$, plunge angle $P_{pl} = 29°$; for the tension axis T, strike azimuth $T_{az} = 252°$, plunge angle $T_{pl} = 1°$; strike azimuth for the axis coinciding with the intersection of two nodal planes $B_{az} = 162°$, plunge angle $B_{pl} = 66°$.

The earthquake hypocentre determined as a result of this study was located into the tectonic structure formed by the *Yantarnensk* fault zone and the zone of the *Bakalinsk* ruptured flexure. This allows the authors to assume the seismotectonic activity of these tectonic structures. The source model of the Kaliningrad earthquake is in agreement with the focal-mechanism solution of other seismological agencies, as well as with the orientation of the above-mentioned tectonic zones, considering the source depth of 3 km.

ACKNOWLEDGEMENT

REFERENCES

Aki, K., Richards, P.G. 1980. *Quantitative Seismology: Theory and Methods*. San Francisco: W.H. Freeman, I, 557 pp.

Ankudinov, S.A., Brio, Kh.S., Sadov, A.S. 1991. Glubinnoye stroyeniye zemnoy kory na territorii respublik Pribaltiki po dannym seysmorazvedochnykh rabot GSZ [Deep structure of the earth's crust in the territory of the Baltic republics according to seismic data from the DSS]. *Belorusskiy seysmologicheskiy byulleten. 1*, 111–117. Minsk: ONTII. [In Russian].

Aptikaev, F.F., Aleshin, A.S., Nikonov, A.A., Pogrebchenko, V.V., E`rteleva, O.O., Assinovskaya, B.A. 2019. Makrosejsmicheskie proyavleniya Kaliningradskogo zemletryaseniya 2014 goda [Macroseismic evidences of the 2004 Kaliningrad earthquake]. *GeoRisk 13 (3)*, 40 – 59. [In Russian].

Assinovskaya, B.A. 2009. Severo-Zapadnaya chast Kaliningradskoy oblasti. Kurshskaya kosa [Northwestern part of the Kaliningrad region. Curonian Spit] *Kaliningradskoye zemletryaseniye 21 sentyabrya 2004 goda*, 88–97. [In Russian].

Assinovskaya, B., Shchukin, J., Gorshkov, V., Shcherbakova, N. 2011. On recent deodynamics of the Eastern Baltic Sea region. *Baltica 24 (2)*, 61–70.

Blazhchizhin, A.I. 1974. Geologicheskoye stroyeniye podvodnogo beregovogo sklona Sambiyskogo poluostrova [Geological structure of the underwater coastal slope of the Sambian peninsula]. *Regionalnaya geologiya Pribaltiki i Belorussii*, 161–168. [In Russian].

Bogdanova, S.V., Bibikova, E.V., Gorbatschev, R. 1994. Palaeoproterozoic U-Pb zircon edges from Belorussia: new geodynamic implications for the East European Craton. *Precambrian Res*earch *68 (1–4)*, 231–240.

David, M. Lucas. 1813. *Preussische Chronik* [*Prussian Chronicle*]. Funfter Band. Konigsberg, 246 pp. [In German].

Dodonov, E.A., Namestnikov, Yu.G., Yakushova, A.F. 1976. *Noveyshaya tektonika yugo-vostoka Baltiyskoy sineklizy* [*The latest tectonics of the southeastern Baltic syneclise*]. Moscow, MGU. 196 pp. [In Russian].

EUROBRIDGE'95 seismic working group, Yliniemi, J., Tiira, T., Luosto, U., Komminaho, K., Giese, R., Motuza, G., Nasedkin, V., Jacyna, J., Seckus, R., Grad, M., Czuba, W., Janik, T., Guterch, A., Lund, C-E., Doody, J.J. 2001. EUROBRIDGE'95: deep seismic profiling within the East European Craton. *Tectonophysics 339*, 153–175.

Ferdinand, R.W., Arvidsson, R. 2002. The determination of source mechanisms of small earthquakes and revised models of local crustal structure by moment tensor inversion. *Geophysical Journal International 151*, 221–234.

Garetsky, R., Levkov, E., Schwab, G., Karabanov, A., Aizberg, R., Garbar, D., Koskel, F., Ludwig, A.O., Lukke-Andersen, H., Ostaficzuk, S., Palienko, V., Sim, L., Sliaupa, A., Sokolowski, J., Stackebrandt, W. 1999. Main neogeodynamic features of the Baltic Sea depression and adjacent areas. *Technika poszukiwan geologicznych. Geosynoptyka i Geotermia 1*, 17–27.

Grigelis, A.A. (ed.). 1981. *Geologiya i geomorfologiya Baltiyskogo morya. Obyasnitelnaya zapiska k geologicheskim kartam masshtaba 1:500000* [*Geology and geomorphology of the Baltic Sea*. Explanatory note to the Geological maps in scale 1:500000]. Nedra, Leningrad, 420 pp. [In Russian].

Godano, M., Bardainne, T., Regnier, M., Deschamps, A. 2011. Moment tensor determination by nonlinear inversion of amplitudes. *Bulletin of the Seismological Society of America 101*, 366–378.

Gorbatikov, A.V., Stepanova, M.Yu., Korablev, G.E. 2008. Zakonomernosti formirovaniya mikroseysmichesko-go polya pod vliyaniyem lokalnykh geologicheskikh neodnorodnostey i zondirovaniye sredy s pomoshchyu mikroseysm [Regularities of the formation of a microseismic field under the influence of local geological inhomogeneities and sounding of the environment using microseisms]. *Fizika Zemli 7*, 66–84. [In Russian].

Gregersen, S., Basham, P.W. (eds) 1989. *Earthquakes at North-Atlantic Passive Margins: Neotectonics and Postglacial Rebound*. Kluwer Academic Publishers, Dordrecht, Netherlands, 716 pp.

Gregersen, S., Wiejacz, P., Debski, W., Domanski, B., Assinovskaya, B. A., Guterch, B., Mäntyniemi, P., Nikulin, V.G., Pacesa, A., Puura, V., Aronov, A. G., Aronova, T.I., Grünthal, G., Husebye, E.S., Sliaupa, S. 2007. The exceptional earthquakes in Kaliningrad district, Russia on September 21, 2004. *Physics of the Earth and Planetary Interiors 164 (1–2)*, 63–74.

Hardebeck, J.L., Shearer, P.M. 2003. Using S/P amplitude ratios to constrain the focal mechanisms of small earthquakes. *Bulletin of the Seismological Society of America 93*, 2432–2444.

Heidbach, O., Tingay, M., Barth, A., Reinecker, J., Kurfeß, D., Müller, B. 2010. Global stress pattern based on the World Stress Map database release 2008. *Tectonophysics 482*, 3–15.

Janutyte, I., Kozlovskaya, E., Motuza, G. and PASSEQ Working Group. 2013. Study of local seismic events in Lithuania and adjacent areas using data from the PASSEQ experiment. *Pure Applied Geophysics 170*, 797–814.

Kondorskaya, N.V., Nikonov, A.A., Ananyin, I.V., Dolgopolov, D.V., Korhonen, H., Arhe, K., Sildvee, H.H. 1988. Osmussaar earthquake in the East Baltics of 1976. *Recent seismological investigation in Europe. Proceedings of the XIX General Assembly of the European Seismological Commission*, 376–387.

Lagerback, R. 1979. Neotectonic structures in Northern Sweden. *Geologiska Föreningens i Stockholm Förhandlingar 100*, 263–269.

Laska, W. 1902. *Die Erdbeben Polens* [*The earthquakes in Poland*]. Mitt. Erdbeben-Comission d. K. Akademie d. Wissenschaften. Neue Folge 8, 36 pp.

Lentas, K. 2018. Towards routine determination of focal mechanisms obtained from first motion P-wave arrivals. *Geophysical Journal International 212 (3),* 1665–1686, doi: 10.1093/gji/ggx503

Lentas, K., Di Giacomo, D., Harris, J., Storchak, D.A. 2019. The ISC Bulletin as a comprehensive source of earthquake source mechanisms. *Earth System Science Data 11*, 565–578, doi: https://doi.org/10.5194/essd-11-565-2019

Lukyanova, N.V., Bogdanov, Yu.B., Vasilyeva, O.V., Vargin, G.P., *et al*. 2011. *Gosudarstvennaya geologicheskaya karta Rossiyskoy Federatsii. Masshtab 1: 1000000 (tretye pokoleniye). Seriya Tsentralno-Evropeyskaya. List N-(34) – Kaliningrad. Obyasnitelnaya zapiska [State geological map of the Russian Federation. Scale 1: 1,000,000 (third generation). Central European series. Sheet N-(34) – Kaliningrad. Explanatory letter]*. VSEGEI, Sankt-Peterburg, 226 pp. + 17 vkl. [In Russian].

Lundqvist, J., Lagerback, R. 1976. The Parvie fault: A late glacial fault in the Precambrian of Swedish Lapland. *Geologiska Föreningens i Stockholm Förhandlingar 98*, 45–51.

Mai, M., Schorlemmer, D., Page, M. *et al*. 2016. The Earthquake-Source Inversion Validation (SIV) Project. *Seismological Research Lett*ers 87, *(3)*, 690–708, doi: 10.1785/0220150231

Malytskyy, D. 2010. Analitychno-chyslovi pidkhody do obchyslennia chasovoi zalezhnosti komponent tenzora seismichnoho momentu [Analytic-numerical approaches to the calculation of seismic moment tensor as a function of time]. *Geoinformatika 1*, 79–86. [In Ukrainian].

Malytskyy, D.V. 2016. *Matematychne modeliuvannia v zadachakh seismolohii* [*Mathematical modelling in the problems of seismology*]. IGF NANU, Kiev, Наукова думка, 241 pp. [In Ukrainian].

Malytskyy, D., Kozlovskyy, E. 2014. Seismic waves in layered media. *Journal of Earth Science and Engineering 4*, 311–325.

Malytskyy, D., D'Amico, S. 2015. *Moment tensor solutions through waveforms inversion*. ISBN: 978-88-98161-13-3, Mistral Service sas, Messina, Italy, 25 pp.

Mazur, S., Mikolajczak, M., Krzywiec, P., Malinowski, M., Buffenmyer, V., Lewandowski, M. 2015. Is the Teisseyre-Tornquist Zone an ancient plate boundary of Baltica? *Tectonics* 34, 2465–2477, doi:10.1002/2015TC003934

Nikonov, A.A. 2007. Approach to parametrization of tectonic earthquakes within the Kaliningrad district, Russia, by macroseismic data. *Seismicity and seismological observations of the Baltic Sea region and adjacent territories*, 57–59.

Nikonov, A.A. 2010. Morozoboynyye sotryaseniya kak osobyy klass seysmicheskikh yavleniy (po materialam-Vostochno-Evropeyskoy platformy) [Frost shaking as a special class of seismic phenomena (based on the materials of the East European platform)]. *Fizika Zemli 3*, 257–273. [In Russian].

Nikulins, V.G. 2007. Regional features of seismotectonics and deformation of Earth crust of the Baltic region. *Seismicity and seismological observations of the Baltic Sea region and adjacent territories*, 63–65.

Nikulins, V. 2017. *Seismicity of the East Baltic region and application-oriented methods in the conditions of low seismicity*. Riga: Latvijas Universitate, Akademiskais apgads, 291 pp.

Nikulins, V. 2020. Seismological Monitoring in Latvia. *Summary of the Bulletin of the International Seismological Centre 54 (I)*, 50–66, https://doi.org/10.31905/BKETRT2R

Ostrovsky, A.A. 1995. Zona drevnego riftoobrazovaniya

pod Baltiyskim morem [Zone of ancient rift formation under the Baltic Sea]. *Doklady Akademii nauk 342 (5)*, 680–685. [In Russian].

Ostrovsky, A.A., Flueh, E.R., Luosto, U. 1994. Deep seismic structure of the Earth's crust along the Baltic Sea profile. *Tectonophysics 233*, 279–292.

Otmas, A.A., Desyatkov, V.M., Chegesov, I.K. 2006. Tektonicheskoye rayonirovaniye Kaliningradskoy oblasti i sopredelnogo shelfa [Tectonic zoning of the Kaliningrad region and adjacent shelf]. *Geologiya, geofizika i razrabotka neftyanykh i gazovykh mestorozhdeniy 8*, 13–24. [In Russian].

Peter iz Duisburga. 1997. *Khronika zemli Prusskoi* [*Chronic of the Prussia Land*]. Ladomir, 384 pp. [In Russian].

Rogozin, E.A., Ovsucenko, A.N., Gorbatikov, A.V., Lutikov, A.I., Novikov, S.S., Marahanov, A.V., Stepanova, M.U., Andreeva, R.V., Larkov, A.S. 2014. Otsenka seysmicheskoy opasnosti g. Kaliningrad v detalnom masshtabe [Seismic hazard assessment for Kaliningrad on a detailed scale]. *Seysmicheskoye stroitelstvo i bezopasnost sooruzheniy 4*, 19–27. [In Russian].

Slunga, R. 1979. Source mechanism of the Baltic earthquake inferred from surface-wave recordings. *Bulletin of the Seismological Society of America 69 (6)*, 1931–1964.

Slunga, R. 1989. Focal mechanisms and crustal stresses in the Baltic Shield. In: Gregersen, S., Basham, P.W. (eds), *Earthquakes at North-Atlantic Passive Margins: Neotectonics and Postglacial Rebound*. Kluwer, Dordrecht, 261–276.

Slunga, R., Norrman, P., Glans, A.-C. 1984. Baltic shield seismicity, the results of a regional network. *Geophysical Research Letters 11 (12)*, 1247–1250.

Stephansson, O., Zang, A. 2012. ISRM suggested methods for rock stress estimation – Part 5: Establishing a model for the in-situ stress at a given site. *Rock Mechanics and Rock Engineering 45 (6)*, 955–969.

Ulomov, V.I., Akatova K.H., Medvedeva N.S. 2008. K otsenke seysmicheskoy opasnosti v Kaliningradskoy oblasti [To the seismic hazard assessment of the Kaliningrad region]. *Fizika Zemli 9*, 3–19. [In Russian].

Vavrychuk, V., Kuhn D. 2012. Momenttensor inversion of waveforms: a two-step time frequency approach. *Geophysical Journal International 190*, 1761–1776.

Vezac, P., Debski, V., Domanski, B., Kapor, D. 2009. Issledovaniye Kaliningradskogo zemletryaseniya 21 sentyabrya 2004 g. instrumentalnymi metodami [Study of the Kaliningrad earthquake on September 21, 2004 by instrumental methods]. *Kaliningradskoye zemletryaseniye 21 sentyabrya 2004 g.*, 45–53. [In Russian].

Weber, Z. 2006. Probabilistic local waveform inversion for moment tensor and hypocentral location. *Geophysical Journal International 165*, 607–621.

Weber, Z. 2016. Probabilistic waveform inversion for 22 earthquake moment tensors in Hungary: new constraints on the tectonic stress pattern inside the Pannonian basin. *Geophysical Journal International 204*, 236–249.

Zagorodnyh, V.A., Dovbnya, A.V., Zhamojda, V.A. et al. 2002. Proizvodstvo geologicheskogo, gidrogeologicheskogo doizucheniya, geologo-ekologicheskih issledovanij i kartografirovaniya territorii Kaliningradskoj oblasti masshtaba 1:200 000. Podgotovka k izdaniyu komplektov gosgeolkarty-200 (novaya seriya): listy N–34-II, - III, - VIII, IX, X, XI, XIV, XV, XVI, XVII [Production of geological, hydrogeological additional study, geological and environmental studies and mapping of the territory of the Kaliningrad region at a scale of 1: 200,000. Preparation for publication of sets of state geological maps-200 (new series): sheets N-34-II, - III, - VIII, IX, X, XI, XIV, XV, XVI, XVII]. Gusev: Kaliningradskaya gidrogeologicheskaya ekspediciya (KGE). SPb: VSEGEI. [In Russian].

Zakarevičius, A., Šliaupa, S., Paršeliūnas, E., Būga, A., Stanionis, A. 2011. The dispersion of horizontal tectonic stresses in the Earth's crust in the Baltic region. *Geodesy and Cartography 37 (2)*, 77–83.